Bioorg. Med. Chem. 32 (2021) 115972

Contents lists available at ScienceDirect

Bioorganic & Medicinal Chemistry

journal homepage: www.elsevier.com/locate/bmc

Design, synthesis and evaluation of 1-benzyl-1*H*-imidazole-5-carboxamide derivatives as potent TGR5 agonists

Shizhen Zhao [a], Xinping Li [a], Le Wang [a], Wenjing Peng [a], Wenling Ye [a], Weiguo Li [a], Yan-Dong Wang [c], Wei-Dong Chen [a,b,*]

[a] Key Laboratory of Receptors-Mediated Gene Regulation and Drug Discovery, People's Hospital of Hebi, School of Medicine, Henan University, Henan, China
[b] Key Laboratory of Molecular Pathology, School of Basic Medical Science, Inner Mongolia Medical University, Hohhot, China
[c] State Key Laboratory of Chemical Resource Engineering, College of Life Science and Technology, Beijing University of Chemical Technology, Beijing, China

ARTICLE INFO

Keywords:
TGR5
TGR5 agonists
Diabetes
Structure-activity relationship

ABSTRACT

TGR5 is emerging as an important and promising target for the treatment of diabetes, obesity and other metabolic syndromes. A series of novel 1-benzyl-1*H*-imidazole-5-carboxamide derivatives was designed, synthesized and evaluated *in vitro* and *in vivo*. The most potent compounds **19d** and **19e** exhibited excellent agonistic activities against hTGR5, which was superior to those of the reference drugs INT-777 and LCA. In addition, compounds **19d** and **19e** exhibited good selectivity against FXR and presented significant glucose-lowering effects in vivo. Compound 19d could stimulate GLP-1 secretion by activating of TGR5.

1. Introduction

Takeda G-protein-coupled receptor 5 (TGR5, GPBAR1, M-BAR, or GPCR19) belongs to a G-protein-coupled receptor (GPCR) for bile acids. The TGR5 receptor is expressed broadly in various tissues including liver, intestine, pancreas, spleen and brown adipose tissue.[1–5] Activation of TGR5 results in the elevation of intracellular cyclic adenosine monophosphate (cAMP) levels, which is recognized as an important intracellular signaling cascades.[6,7] TGR5 activation has also elevated glucagon like peptide-1 (GLP-1) secretion, which activates intestinal cell secretion and plays a key role in glucose metabolism and energy homeostasis.[8,9] In addition, TGR5 activation increases energy expenditure and oxygen consumption in brown adipose tissue and muscle.[10] Therefore, TGR5 has become an attractive therapeutic target for the treatment of metabolic disorders, such as non-alcoholic steatohepatitis, type 2 diabetes mellitus (T2DM) and obesity.[11–13]

Two categories of TGR5 agonists (steroidal and nonsteroidal) have been discovered in the literature by pharmaceutical companies (Fig. 1). One series is structurally based on bile acids (BAs), including cholic acid (CA), lithocholic acid (LCA) and their semisynthetic derivatives such as 6α-ethyl-23(*S*)-methylcholic acid (INT-777, **1**).[14,15] INT-777 is a selective TGR5 agonist as an antidiabetic drug candidate. In addition, several other nonsteroidal TGR5 agonists have been reported in the literature (**2**–**5**), which exhibited excellent TGR5 agonist activity and were orally efficacious in lowering glucose levels in vivo.[16–22] However, none of these agonists have been successful in clinical trials.

In our effort to discover more potent TGR5 agonists for a treatment of metabolic disease. A number of compounds in our library were evaluated for their TGR5 agonist activity by computer-aided drug design (CADD). Compound **6,** which features 1- benzyl-1*H*-imidazole-5-carboxamide scaffolds, was displayed obvious TGR5 agonist activity, with the EC_{50} values of 19.5 μM. The chemical scaffold of compound **6** is an attractive starting point for generating novel TGR5 agonists. In order to further explore the structure–activity relationships (SARs) and improve TGR5 agonist activity, a series of 1-benzyl-1*H*-imidazole-5-carboxamide derivatives have been synthesized and evaluated for their *in vitro* TGR5 agonist activity.

2. Results and discussion

2.1. Chemistry

The key intermediates **12** was synthesized according to the procedure which were previously reported in Scheme 1.[23] 2-fluoronitrobenzene **7** was used as the starting material, and treated with cyclopropylamine to obtain intermediate **8**. The intermediate **8** was

* Corresponding author at: Key Laboratory of Receptors-Mediated Gene Regulation and Drug Discovery, People's Hospital of Hebi, School of Medicine, Henan University, Henan, China.
E-mail address: wdchen666@163.com (W.-D. Chen).

https://doi.org/10.1016/j.bmc.2020.115972
Received 14 October 2020; Received in revised form 20 December 2020; Accepted 21 December 2020
Available online 27 December 2020

treated with methyl oxalyl chloride in the presence of triethylamine by acylation to produce the intermediate **9**. Further transformation of **9** by reduction reaction to afford **10**, which on treatment with triphenylphosphine provided the intermediate **11**. Finally, intermediate **11** was reduced with borane-tetrahydrofuran complex to obtain the key intermediates **12**.

The target compounds **15a-p** were synthesized as shown in Scheme 2. The intermediate **14** was synthesized from etomidate **13** via hydrolysis reaction with 2 N NaOH. Then, the intermediates **14** reacted with the key intermediate **12**, substituted aniline, substituted *N*-methylaniline or substituted 1-phenylpiperazine in the presence of HATU, that gave the target compounds **15a-p**.

The target compounds **19a-f** were formed according to the reaction pathways illustrated in Scheme 3. Ethyl 1*H*-imidazole-5-carboxylate **16** was used as the starting material, and treated with substituted benzyl bromide by nucleophilic substitution to obtain intermediate **17a-f**. Similar to the preparation of **15a-s,** compounds **19a-f** were synthesized from intermediate **17a-f** by hydrolysis and condensation reactions.

2.2. In vitro biological evaluation

The target compounds were evaluated for their ability to activate hTGR5 by assessing for intracellular levels of cAMP, which used the homogeneous time resolved fluorescence (HTRF) assay, similar to the reported in the literature.[24,25] As reference compound, the response of LCA at 10 μM was defined as 100% hTGR5 activation. Vehicle control with 0.1% DMSO was set to 0% hTGR5 activation. As shown in Table 1, the introduction of different the side chain amide had a notable influence on the hTGR5 activity.

Many of these compounds were found to have agonistic activities against hTGR5 at the concentration of 10 μM and 40 μM. Interestingly, compounds such as 4-F aniline (**15a**), *N*-methyl aniline (**15g, 15h** and **15i**), substituted 1-Phenylpiperazine (**15k** and **15l**) and tetrahydroquinoxaline (**15n**) exhibited agonistic activities with an *Agonistic rate* more then 50% at 10 μM. Furtherly, the most potent compounds **15h, 15k, 15l** and **15n** were evaluated using a dose–response experiment and displayed obvious TGR5 agonist activity, with the EC_{50} values of 1.05, 1.09, 4.39 and 0.33 μM, respectively.

Based on the results above, we selected a scaffold of tetrahydroquinoxaline **15n** as our starting point for further modification. Our optimized efforts were directed toward replacing the phenylethyl group with the substituted benzyl group to expand the SAR studies (Table 2). Most of the compounds (**19a-f**) exhibited excellent hTGR5 agonist activity with EC_{50} values in the range of 6.8 to 1751 nM, which are superior or comparable to those of the reference drug **INT-777**. Of these, Compounds **19d** and **19e** with 2,4-di-Cl and 2,5-di-Cl substituents showed the best hTGR5 agonist activity, with EC_{50} values of 6.8 and 9.5 nM on hTGR5, respectively.

Several potent hTGR5 agonists were further evaluated for their ability to activate mTGR5 using a similar method described for hTGR5 (Table 2). Compared with hTGR5 agonism activity, most of the compounds showed less agonist activity on mTGR5. The differences in potencies may be mainly due to the weak sequence homology (83%) between the two species. Among these, the potent compounds **19d** and **19e**, with EC_{50} values of 611 and 832 nM toward mTGR5 in our assay, respectively. The CLogP values of these compounds are shown in Table 2. Interestingly, there was a increase in TGR5 agonist activity along with increasing *lipophilicity* within compounds **19a-f**.

2.3. FXR activity assay

Because many bile acid derived TGR5 agonists can also activate the nuclear bile acid receptor FXR (Farnesoid X Receptor).[26,27] The most potent compounds **19d** and **19e** were further evaluated by using homogeneous time resolved fluorescence (HTRF) assay. As shown in Table 3, compounds **19d** and **19e** exhibited good selectivity against FXR.

2.4. In vitro human plasma stability assay

The stability of compounds in human plasma is an important consideration in drug discovery. Based on their *in vitro* activities, the most potent compounds **19d** and **19e** were incubated with human Plasma.[24] As shown in Table 4, compounds **19d** and **19e** exhibited excellent metabolic profiles in human plasma at 120 min (remaining 104.0% and105.4%, respectively).

2.5. In vitro cytotoxicity assay

The most potent compounds **19d** and **19e** were further evaluated for their *in vitro* cytotoxicity against A549 and Hela cells. Cytotoxicity was measured using the CCK8 assay after incubation with the compounds for 24 h. As shown in Table 5, Compounds **19d** and **19e** showed no activities toward tumor cell lines A549 and Hela with $IC_{50} > 50$ μM.

2.6. Oral glucose tolerance test in mice

An oral glucose tolerance test (OGTT) was carried out in C57 BL/6

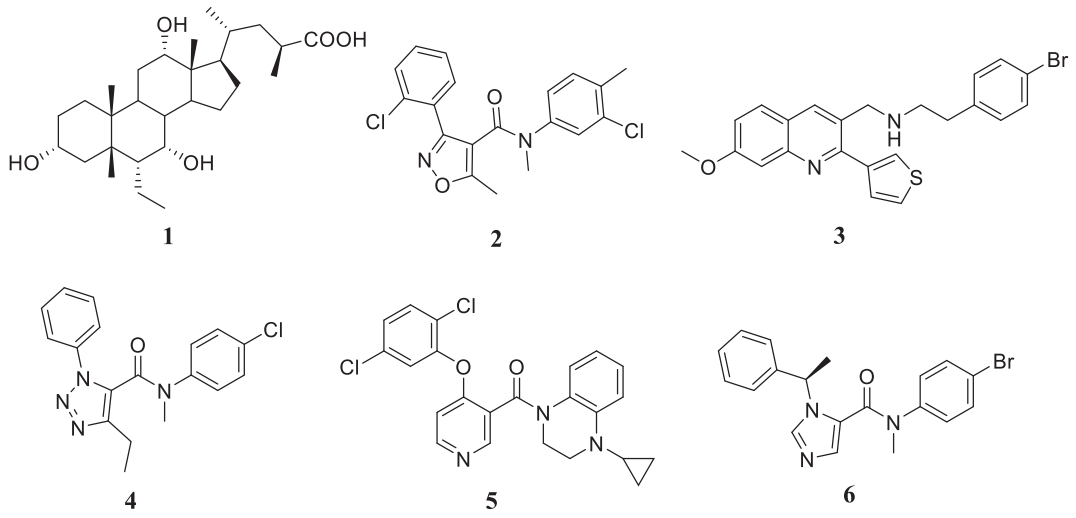

Fig. 1. Structures of some known TGR5 agonists.

mice to examine the effect of compounds **19d** and **19e** on blood glucose (Fig. 2). Mice were fasted overnight before glucose tolerance tests. Compounds **19d** and **19e** at 30 mg/kg were orally administered 60 min prior to the administration of 2 g/kg of glucose. Blood glucose was measured at 0, 15, 30, 60 and 120 min after glucose administration. As shown in Fig. 2, compounds **19d** and **19e** caused a significant 15.8% and 13.7% of reduction in blood glucose $AUC_{0-120\ min}$ compared with the control group.

2.7. GLP-1 secretion

To explore whether the glucose-lowering effect of compound **19d** is dependent on mediated GLP-1 secretion, a further GLP-1 levels of C57 BL/6 mice (WT) and $TGR5^{-/-}$ mice were detected by GLP-1(7–36) ELISA assay. As shown in Fig. 3, compound **19d** could increased the secretion of GLP-1 compared to control in WT mice. In $TGR5^{-/-}$ mice, there is no significant difference for GLP-1 concentration between control and compound **19d** treated groups. All of these results indicated that compound **19d** could stimulate GLP-1 secretion by activating of TGR5.

3. Conclusion

In summary, we have designed and synthesized a series of novel 1-benzyl-1*H*-imidazole-5-carboxamide derivatives as potent TGR5 agonists. Many of these compounds showed agonistic activities against TGR5 at the concentration of 10 μM and 40 μM. Among these, compounds **19d** and **19e** displayed the most remarkable agonistic activities against TGR5, which was superior to those of the reference drugs INT-777 and LCA. In addition, compounds **19d** and **19e** exhibited good selectivity against FXR and presented significant glucose-lowering effects in vivo studies. The GLP-1 ELISA assay indicated that compound **19d** could stimulate GLP-1 secretion by activation of TGR5 in WT and $TGR5^{-/-}$ mice. Further developments of compounds **19d** and **19e** are ongoing in our laboratory.

4. Experimental section

4.1. General procedure for the synthesis of compounds

Unless otherwise noted, all reagents and solvents were obtained from commercially available sources and were used without purification. TLC analysis was performed on GF254 silica gel plates (Jiangyou, Yantai). Column chromatography was carried out with silica gel (200–300 mesh) from Qingdao Haiyang Chemicals (Qingdao, Shandong, China). Mass spectrometry was performed using ESI mode on an Agilent 1200 LC-MS (Agilent, Palo Alto, CA, USA). High-resolution accurate mass determinations (HRMS) were recorded on a Bruker Micromass Time of Flight mass spectrometer equipped with electrospray ionisation (ESI). Nuclear magnetic resonance (^{1}H-NMR and ^{13}C NMR) spectra were recorded on a Bruker 400 MHz NMR spectrometer with TMS as an internal standard. The chemical shifts were reported in parts per million (ppm), the coupling constants (*J*) were expressed in hertz (Hz). Peak multiplicities were described as singlet (s), doublet (d), triplet (t), quartet (q), multiplet (m) and broad (br).

4.2. Cyclopropyl-(2-nitro-phenyl)-amine (8)

Cyclopropylamine (27.31 g, 478.38 mmol) was added to a solution of 2-fluoronitrobenzene (30.00 g, 212.6 mmol), and the resulting mixture was stirred for 12 h at ambient temperature. After confirming that the reaction was complete by using TLC analysis, and the reaction was extracted with ethyl acetate and washed with saturated sodium bicarbonate. The organic layer was dried over anhydrous Na_2SO_4 and concentrated. The crude product was purified by silica gel column chromatography to yield the target product **8** (34.20 g, yield: 90.3%).

4.3. N-Cyclopropyl-N-(2-nitro-phenyl)-oxalamic Acid methyl ester (9)

Methyl oxalyl chloride (23.37 g, 190.8 mmol) was slowly added to a solution of cyclopropyl-(2-nitro-phenyl)-amine (34.00 g, 190.8 mmol) and triethylamine (31.83 mL, 228.9 mmol) in dichloromethane cooled to <0 °C using a salted ice bath. The reaction mixture was stirred at ambient temperature for 12 h. The reaction mixture was extracted with EtOAc and brine. The organic phase was dried over Na_2SO_4 overnight and the solvent was removed under vacuum to give the target product **9** (42.60 g, yield: 84.5%).

4.4. 1-Cyclopropyl-4-hydroxy-1,4-dihydro-quinoxaline-2,3-dione (10)

To a solution of **9** (40.00 g, 151.4 mmol) in methanol (200 mL) was added palladium on carbon (4.00 g, 10%w/w). The reaction flask was evacuated under vacuum and back filled with hydrogen 3 times, before being stirred under a hydrogen atmosphere at ambient temperature for 18 h. The reaction mixture was diluted with ethyl acetate (400 mL), filtered and the solvent was removed in vacuo to give the target product **10** (28.42 g, yield: 86.0%).

4.5. 1-Cyclopropyl-1,4-dihydro-quinoxaline-2,3-dione (11)

A solution of 1-Cyclopropyl-4-hydroxy-1,4-dihydro-quinoxaline-2,3-

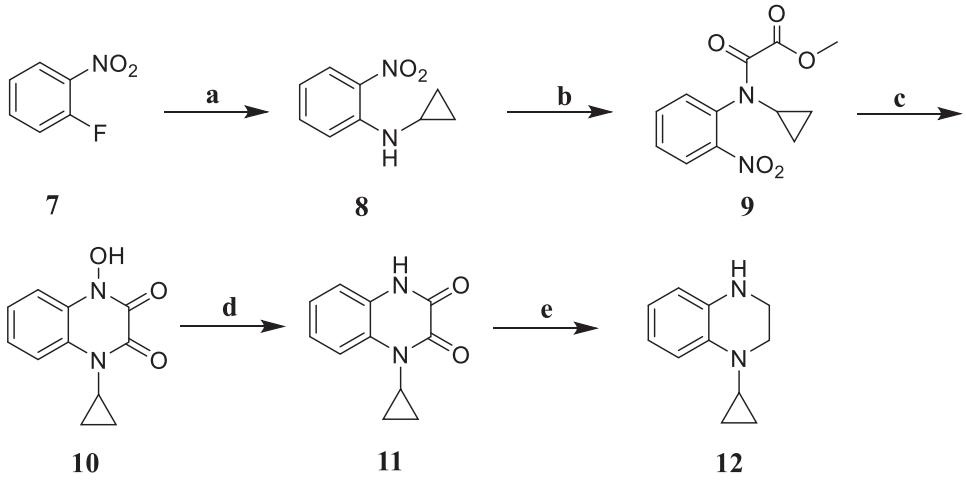

Scheme 1. Synthesis of intermediates **12**. Reagents and conditions:(a) Cyclopropylamine, r.t.; (b) Methyl Oxalyl chloride, Triethylamine, CH_2Cl_2, r.t.; (c) Pd/C, H_2, MeOH, r.t.; (d) Triphenylphosphine, DMF, 135 °C; (e) BH_3-THF, THF, r.t..

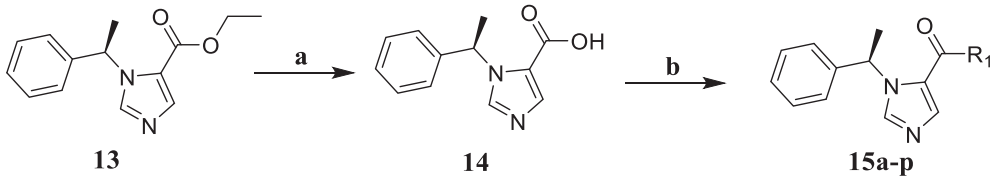

Scheme 2. General synthesis of the target compounds **15a-p**. Reagents and conditions: (a) NaOH, MeOH/H_2O, r.t.; (b) **12**, substituted aniline, substituted *N*-methylaniline or substituted 1-phenylpiperazine, HATU, DIEA, DMF, r.t..

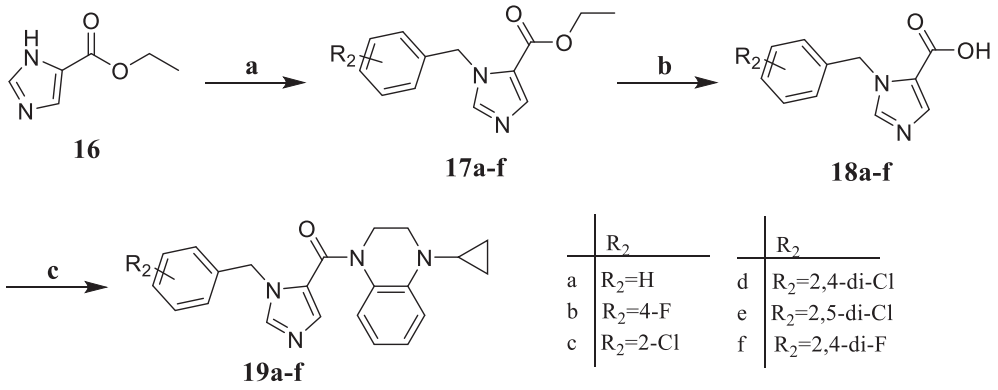

Scheme 3. General synthesis of the target compounds **19a-f**. Reagents and conditions: (a) 10% NaOH, THF, 0 °C; (b) 2 N NaOH, MeOH/H_2O; (c) **12**, HATU, DIEA, DMF, r.t..

dione (28.00 g, 128.3 mmol) and triphenylphosphine (50.48 g, 192.47 mmol) in DMF was heated to 135 °C for 6 h. After confirming that the reaction was complete by using TLC analysis, the solution was cooled to room temperature and dichloromethane (400 mL) was added. The suspension was stirred for 30 min, filtered and washed with dichloromethane to give the desired compound **11** (21.10 g, yield: 81.3%). ^{1}H NMR (300 MHz, DMSO-d_6) δ 11.92 (s, 1H), 7.63 (dd, J = 6.5, 1.8 Hz, 1H), 7.30–7.10 (m, 3H), 2.99–2.86 (m, 1H), 1.30–1.14 (m, 2H), 0.81–0.66 (m, 2H).

4.6. 1-Cyclopropyl-1,2,3,4-tetrahydro-quinoxaline (12)

1 M solution of boranete-trahydrofuran complex (207.8 mL, 207.8 mmmol) was slowly added dropwise to a solution of 1-cyclopropyl-1,4-dihydro-quinoxaline-2,3-dione (21.00 g, 103.9 mmol) in THF (500 mL), and the resulting mixture was stirred for 18 h at ambient temperature. The solvent was removed under reduced pressure, and the residue was extracted with ethyl acetate and washed with brine. The organic layer was dried over anhydrous Na_2SO_4 and concentrated. The crude product was purified by silica gel column chromatography to yield the target product **12** as a white solid (8.60 g, yield: 47.5%). ^{1}H NMR (300 MHz, DMSO-d_6) δ 6.90 (d, J = 7.6 Hz, 1H), 6.57–6.32 (m, 3H), 5.47 (s, 1H), 3.29–3.27 (m, 2H), 3.14–3.12 (m, 2H), 2.14–2.12 (m, 1H), 0.76–0.74 (m, 2H), 0.47–0.45 (m, 2H).

4.7. (R)-1-(1-phenylethyl)-1H-imidazole-5-carboxylic acid (14)

To a solution of etomidate **13** (1.0 g, 4.09 mmol) in methanol was added 2 N sodium hydroxide (5 mL) at ambient temperature. The reaction mixture was stirred for 6 h and the methanol was removed by rotary evaporation. The resultant mixture was adjusted to pH = 5–6 with 1 N HCl. The precipitated white solid was collected by filtration and dried to give the carboxylic acid intermediate **14** (0.81 g, yield: 91.5%).

4.8. General procedure for the synthesis of compounds 15a-p

HATU (1.1 equiv.) and DIEA (2 equiv.) were added to a solution of (*R*)-1-(1-phenylethyl)-1H-imidazole-5-carboxylic acid **14** (1 equiv.) and substituted aniline (1 equiv.) in anhydrous DMF. The solution was heated to 70 °C for 6 h and then cooled to room temperature. The reaction mixture was poured into ice water, and the resulting solid was filtered. The crude product was purified by silica gel column chromatography to give the target product **15a-p**.

4.8.1. (R)-N-(4-fluorophenyl)-1-(1-phenylethyl)-1H-imidazole-5-carboxamide (15a)

Light white solid; yield: 72.8%; ^{1}H NMR (400 MHz, DMSO-d_6) δ 10.09 (s, 1H), 8.22 (s, 1H), 7.77 (s, 1H), 7.69–7.60 (m, 2H), 7.32 (t, J = 7.4 Hz, 2H), 7.25 (d, J = 7.3 Hz, 1H), 7.23–7.19 (m, 2H), 7.15 (t, J = 8.9 Hz, 2H), 6.40 (q, J = 7.2 Hz, 1H), 1.85 (d, J = 7.3 Hz, 3H). ^{13}C NMR (100 MHz, DMSO-d_6) δ 158.6, 157.1, 142.6, 139.8, 135.0, 133.6, 128.6 (2C), 127.6, 126.0 (2C), 125.0, 122.1, 122.0, 115.4 , 115.1, 54.3, 21.7. HRMS calcd for $C_{18}H_{17}FN_3O$, $[M + H]^+$, 310.1356; found 310.1349

4.8.2. (R)-N-(3-fluorophenyl)-1-(1-phenylethyl)-1H-imidazole-5-carboxamide (15b)

Light white solid; yield: 75.1%; ^{1}H NMR (400 MHz, DMSO) δ 10.20 (s, 1H), 8.25 (s, 1H), 7.80 (s, 1H), 7.60 (d, J = 11.8 Hz, 1H), 7.43 (d, J = 8.4 Hz, 1H), 7.39–7.29 (m, 3H), 7.23 (dd, J = 17.5, 7.2 Hz, 3H), 6.90 (td, J = 8.4, 2.2 Hz, 1H), 6.39 (q, J = 7.2 Hz, 1H), 1.86 (d, J = 7.2 Hz, 3H). ^{13}C NMR (101 MHz, DMSO) δ 163.7, 159.2, 143.0, 141.0, 140.5, 134.5, 130.8, 129.1(2C), 128.0, 126.5 (2C), 125.6, 116.2, 110.4, 107.4, 54.8, 22.1.HRMS calcd for $C_{18}H_{17}FN_3O$, $[M + H]^+$, 310.1356; found 310.1351.

4.8.3. (R)-N-(2-fluorophenyl)-1-(1-phenylethyl)-1H-imidazole-5-carboxamide (15c)

Light white solid; yield: 73.2%; ^{1}H NMR (400 MHz, DMSO-d_6) δ 9.90 (s, 1H), 8.24 (s, 1H), 7.82 (s, 1H), 7.47 (t, J = 7.7 Hz, 1H), 7.32 (t, J = 7.3 Hz, 2H), 7.28–7.14 (m, 6H), 6.41 (q, J = 7.2 Hz, 1H), 1.84 (d, J = 7.3 Hz, 3H). ^{13}C NMR (101 MHz, DMSO) δ 159.1, 157.4, 142.9, 140.3, 134.45, 129.0 (2C), 128.0, 127.6, 127.4, 126.5 (2C), 125.4, 125.2, 124.7, 116.2, 54.7, 22.1. HRMS calcd for $C_{18}H_{17}FN_3O$, $[M + H]^+$, 310.1356; found 310.1343.

Table 1

In vitro biological evaluation.[a]

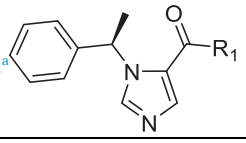

Compd.	R_1	Agonistic rate at 10μM (%)	Agonistic rate at 40μM (%)	hTGR5 EC_{50} (μM)[b]
15a	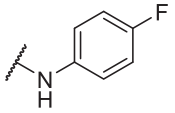	51.29	85.21	–
15b	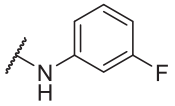	20.14	56.18	–
15c	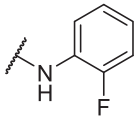	16.52	48.40	–
15d	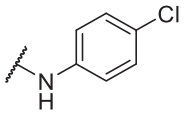	37.71	84.13	–
15e	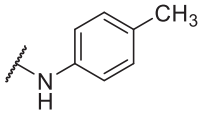	20.16	63.33	–
15f	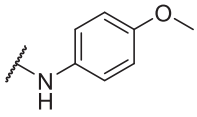	25.34	66.51	–
15g	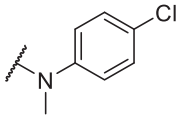	63.13	71.88	–
15h	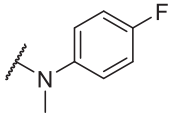	70.88	85.36	1.05±0.21
15i	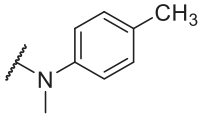	62.12	86.67	–
15j	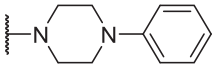	41.72	81.64	–
15k	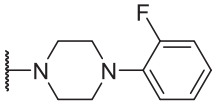	79.34	95.34	1.09±0.11
15l	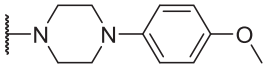	79.08	89.65	4.39±0.16
15m	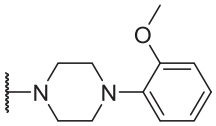	17.39	49.18	–
15n		89.79	97.36	0.33±0.08

(*continued on next page*)

Table 1 (*continued*)

Compd.	R_1	Agonistic rate at 10μM (%)	Agonistic rate at 40μM (%)	hTGR5 EC_{50} (μM)[b]
15o	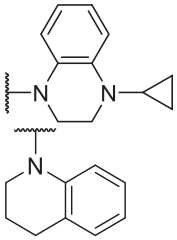	48.32	77.14	–
15p	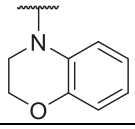	54.12	74.53	–

[a] The response to 10 μM LCA was set to 100% and 0.1% DMSO was set to 0% hTGR5 activation. Data represent mean of three independent experiments. EC_{50} values given are expressed as mean ± SEM of three independent experiments.
[b] –, not tested.

Table 2

In vitro biological evaluation.[a]

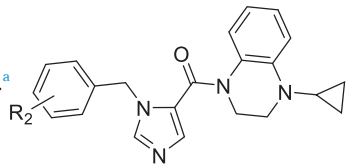

Compd.	R_2	hTGR5 EC_{50} (nM)	mTGR5 EC_{50} (nM)	CLogP[b]
19a	H	1751 ± 52	3500 ± 35	2.99
19b	4-F	568 ± 68	>10,000	3.13
19c	2-Cl	118 ± 11	3690 ± 86	3.70
19d	2,4-di-Cl	6.8 ± 0.43	611 ± 33	4.42
19e	2,5-di-Cl	9.5 ± 0.61	832 ± 47	4.42
19f	2,4-di-F	338 ± 21	>10,000	3.28
INT-777		820 ± 43	132 ± 24	
5		2.8 ± 0.19	3.2 ± 0.09	

[a] EC_{50} values given are expressed as mean ± SEM of three independent experiments.
[b] Calculated from ChemBioDraw Ultra 12.0 by CambridgeSoft.

Table 3
FXR Agonistic activities of the compounds **19d** and **19e** by HTRF assay.[a]

Compd.	FXR (% effect at 10μM)	FXR (% effect at 20μM)	FXR (% effect at 50μM)
19d	1.1	1.6	−1.1
19e	2.3	−0.8	0.31
CDCA	–	–	100%

[a] The response to 50 μM CDCA was set to 100% and 0.1% DMSO was set to 0% FXR activation. – , not tested.

Table 4
In vitro human Plasma Stability of compounds **19d** and **19e**.

Compd.	Stablity in Human Blood Plasma	
	% Remaining at 60min	% Remaining at 120min
19d	107.2	104.0
19e	111.6	105.4

*4.8.4. (R)-N-(4-chlorophenyl)-1-(1-phenylethyl)-1H-imidazole-5-carboxamide (**15d**)*

Light white solid; yield: 75.9%; ^{1}H NMR (400 MHz, $CDCl_3$) δ 7.99 (s, 1H), 7.71 (d, J = 11.9 Hz, 2H), 7.50 (d, J = 8.9 Hz, 2H), 7.32 (ddd, J = 11.8, 8.6, 6.7 Hz, 5H), 7.25–7.21 (m, 2H), 6.49 (q, J = 7.1 Hz, 1H), 1.88 (d, J = 7.1 Hz, 3H). ^{13}C NMR (100 MHz, DMSO-d_6) δ 158.6, 142.6, 139.9, 137.7, 133.9, 128.6 (2C), 128.6 (2C), 127.5, 127.2, 126.0 (2C), 125.2, 121.7 (2C), 54.4, 21.7. HRMS calcd for $C_{18}H_{17}ClN_3O$, $[M + H]^+$, 326.1060; found 326.1062.

Table 5
In vitro cytotoxicity of compounds on A549 and Hela cells.

Compd.	IC_{50} (μM)[a]	
	A549	Hela
19d	>50	>50
19e	>50	>50

[a] The mean values of three independent experiments ± SE are reported.

*4.8.5. (R)-1-(1-phenylethyl)-N-(p-tolyl)-1H-imidazole-5-carboxamide (**15e**)*

Light white solid; yield: 72.5%; ^{1}H NMR (400 MHz, DMSO-d_6) δ 9.94 (s, 1H), 8.20 (s, 1H), 7.75 (s, 1H), 7.51 (d, J = 8.4 Hz, 2H), 7.32 (t, J = 7.3 Hz, 2H), 7.25 (d, J = 7.1 Hz, 1H), 7.21 (d, J = 7.2 Hz, 2H), 7.11 (d, J = 8.3 Hz, 2H), 6.42 (q, J = 7.2 Hz, 1H), 2.25 (s, 3H), 1.85 (d, J = 7.3 Hz, 3H). ^{13}C NMR (100 MHz, DMSO-d_6) δ 158.5, 142.6, 139.6, 136.1, 133.4, 132.6, 129.0 (2C), 128.6 (2C), 127.5, 126.0 (2C), 125.5, 120.2 (2C), 54.2, 21.7, 20.5. HRMS calcd for $C_{19}H_{20}N_3O$, $[M + H]^+$, 306.1606; found 306.1600.

*4.8.6. (R)-N-(4-methoxyphenyl)-1-(1-phenylethyl)-1H-imidazole-5-carboxamide (**15f**)*

Light white solid; yield: 66.5%; ^{1}H NMR (400 MHz, DMSO-d_6) δ 9.93 (s, 1H), 8.19 (s, 1H), 7.75 (s, 1H), 7.58–7.50 (m, 2H), 7.32 (t, J = 7.3 Hz, 2H), 7.27–7.18 (m, 3H), 6.89 (d, J = 9.0 Hz, 2H), 6.44 (q, J = 7.2 Hz, 1H), 3.73 (s, 3H), 1.85 (d, J = 7.3 Hz, 3H). ^{13}C NMR (101 MHz, DMSO-d_6) δ 158.4, 155.5, 142.7, 139.5, 133.2, 131.7, 128.6 (2C), 127.5, 126.0 (2C), 125.5, 121.9 (2C), 113.8 (2C), 55.2, 54.2, 21.7.HRMS calcd for $C_{19}H_{20}N_3O_2$, $[M + H]^+$, 322.1556; found 322.1554.

*4.8.7. (R)-N-(4-chlorophenyl)-N-methyl-1-(1-phenylethyl)-1H-imidazole-5-carboxamide (**15g**)*

Light white solid; yield: 60.5%; ^{1}H NMR (400 MHz, DMSO-d_6) δ 8.00 (s, 1H), 7.41 (t, J = 7.5 Hz, 2H), 7.33 (t, J = 7.2 Hz, 1H), 7.26 (d, J = 8.5 Hz, 2H), 7.17 (d, J = 7.6 Hz, 2H), 6.67 (d, J = 8.4 Hz, 2H), 6.37 (s, 1H), 6.01 (q, J = 7.2 Hz, 1H), 3.19 (s, 3H), 1.83 (d, J = 7.2 Hz, 3H). ^{13}C NMR (100 MHz, DMSO-d_6) δ 160.9, 143.2, 142.5, 137.5, 133.7, 131.3, 129.1, 128.7, 128.6, 127.9, 126.3 (2C), 125.4, 54.7, 37.2, 21.2. HRMS calcd for

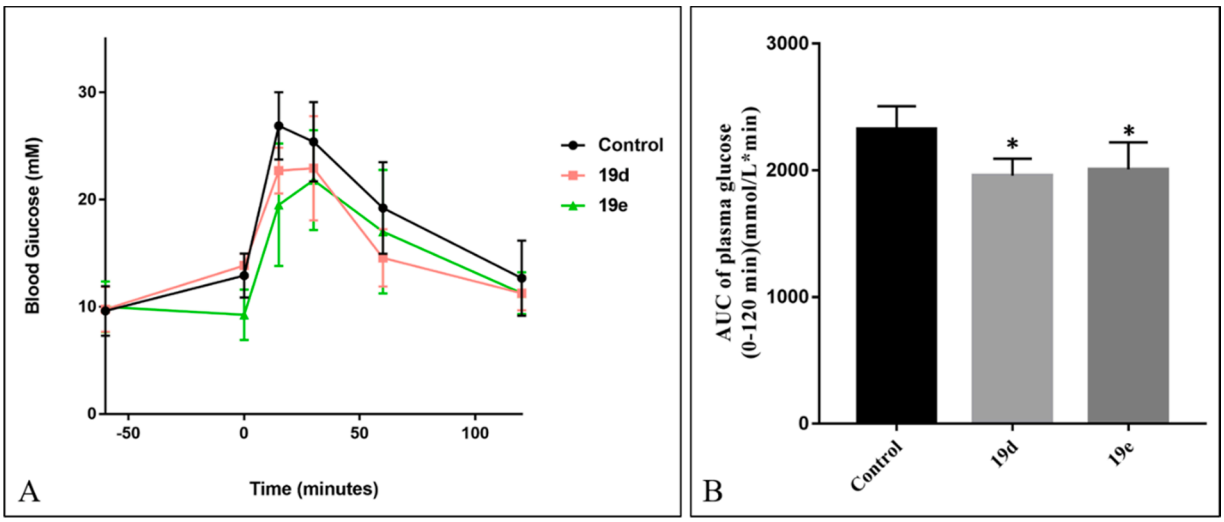

Fig. 2. Oral glucose tolerance test (OGTT) of compounds **19d** and **19e** in male C57BL/6 mice. (A) Blood glucose concentration; (B) blood glucose $AUC_{0-120\ min}$. Compounds **19d** and **19e** (30 mg/kg in 0.25%CMC) or 0.25% CMC (Control) was orally administered at −60 min of OGTT followed by oral glucose challenge at 2.0 g/kg at 0 min. n = 7–8 animals/group. *P < 0.05 vs. control. Error bar indicates SEM (standard error of the mean).

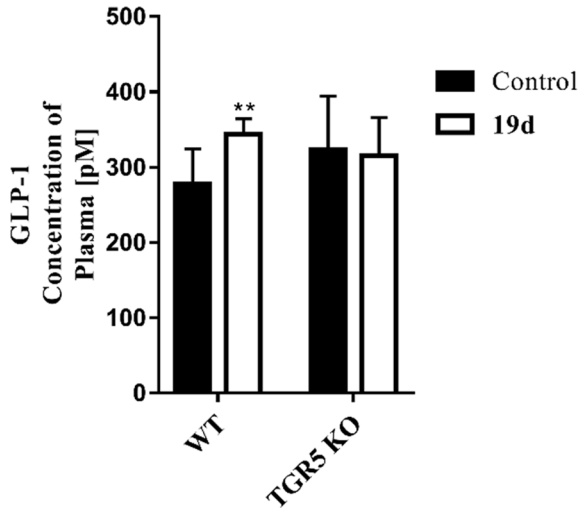

Fig. 3. *In vivo* GLP-1 secretion study of compound **19d** at 30 mg/kg in C57 BL/6 mice (WT) and $TGR5^{-/-}$ mice (TGR5 KO). n = 7–8 animals/group. **P < 0.01 vs. control. Error bar indicates SEM.

$C_{19}H_{19}ClN_3O$, $[M + H]^+$, 340.1217; found 340.1218.

*4.8.8. (R)-N-(4-fluorophenyl)-N-methyl-1-(1-phenylethyl)-1H-imidazole-5-carboxamide (**15h**)*

Light white solid; yield: 69.5%; ^{1}H NMR (400 MHz, DMSO-d_6) δ 7.98 (s, 1H), 7.40 (t, J = 7.3 Hz, 2H), 7.33 (dd, J = 8.4, 6.0 Hz, 1H), 7.16 (d, J = 7.1 Hz, 2H), 7.05 (t, J = 8.8 Hz, 2H), 6.71 (dd, J = 8.4, 5.0 Hz, 2H), 6.33 (s, 1H), 6.02 (q, J = 7.1 Hz, 1H), 3.18 (s, 3H), 1.83 (d, J = 7.2 Hz, 3H). ^{13}C NMR (100 MHz, DMSO-d_6) δ 161.1, 142.6, 140.6, 140.6, 137.4, 133.5, 129.0, 128.9, 128.7 (2C), 127.9, 126.4 (2C), 125.4, 116.1, 115.8, 54.7, 37.5, 21.2. HRMS calcd for $C_{19}H_{19}FN_3O$, $[M + H]^+$, 324.1512; found 324.1513.

*4.8.9. (R)-N-methyl-1-(1-phenylethyl)-N-(p-tolyl)-1H-imidazole-5-carboxamide (**15i**)*

Light white solid; yield: 71.7%; ^{1}H NMR (300 MHz, DMSO-d_6) δ 7.96 (s, 1H), 7.36 (dq, J = 14.3, 7.1 Hz, 3H), 7.16 (d, J = 6.9 Hz, 2H), 7.00 (d, J = 8.1 Hz, 2H), 6.54 (d, J = 8.0 Hz, 2H), 6.28 (s, 1H), 6.06 (q, J = 7.3 Hz, 1H), 3.17 (s, 3H), 2.23 (s, 3H), 1.82 (d, J = 7.2 Hz, 3H). ^{13}C NMR (100 MHz, DMSO-d_6) δ 161.0, 142.6, 141.8, 137.2, 136.5, 133.5, 129.7 (2C), 128.7 (2C), 127.8, 126.6 (2C), 126.4 (2C), 125.6, 54.6, 37.4, 21.2, 20.5. HRMS calcd for $C_{20}H_{22}N_3O$, $[M + H]^+$, 320.1763; found 320.1759.

*4.8.10. (R)-(1-(1-phenylethyl)-1H-imidazol-5-yl)(4-phenylpiperazin-1-yl) methanone (**15j**)*

Light white solid; yield: 74.8%; ^{1}H NMR (400 MHz, DMSO-d_6) δ 8.12 (s, 1H), 7.28 (t, J = 7.6 Hz, 2H), 7.23–7.16 (m, 4H), 7.10 (d, J = 7.2 Hz, 2H), 6.85 (d, J = 8.0 Hz, 2H), 6.80 (t, J = 7.3 Hz, 1H), 5.77 (q, J = 7.1 Hz, 1H), 3.39–3.34 (m, 4H), 2.94–2.89 (m, 4H), 1.83 (d, J = 7.2 Hz, 3H). ^{13}C NMR (100 MHz, DMSO-d_6) δ 160.4, 150.7, 142.6, 137.7, 130.7, 129.0 (2C), 128.7 (2C), 127.6, 126.1 (2C), 124.9, 119.5, 116.0 (2C), 56.0, 54.8 (2C), 48.3 (2C), 21.2. HRMS calcd for $C_{20}H_{22}N_3O_3SNa$, $[M + Na]^+$, 383.1848; found 383.1842.

*4.8.11. (R)-(4-(2-fluorophenyl)piperazin-1-yl)(1-(1-phenylethyl)-1H-imidazol-5-yl)methanone (**15k**)*

Light white solid; yield: 68.2%; ^{1}H NMR (400 MHz, $CDCl_3$) δ 7.79 (s, 1H), 7.22 (dd, J = 13.2, 5.5 Hz, 2H), 7.15 (t, J = 7.3 Hz, 1H), 7.10 (s, 1H), 7.04 (d, J = 7.2 Hz, 2H), 7.01–6.96 (m, 1H), 6.97–6.85 (m, 2H), 6.77–6.64 (m, 1H), 5.86 (q, J = 7.1 Hz, 1H), 3.85–3.31 (m, 4H), 2.72–2.70 (m, 4H), 1.81 (d, J = 7.1 Hz, 3H). ^{13}C NMR (100 MHz, DMSO-d_6) δ 160.4, 142.6, 139.4, 137.7, 130.6, 128.7 (2C), 127.7, 126.1 (2C), 124.9, 124.8, 123.0, 119.5, 116.1, 115.9, 54.9, 49.9 (2C), 49.9 (2C), 21.2. HRMS calcd for $C_{22}H_{24}FN_4O$, $[M + H]^+$, 379.1934; found 379.1947.

*4.8.12. (R)-(4-(4-methoxyphenyl)piperazin-1-yl)(1-(1-phenylethyl)-1H-imidazol-5-yl)methanone (**15l**)*

Light white solid; yield: 74.4%; ^{1}H NMR (400 MHz, DMSO-d_6) δ 8.55 (s, 1H), 7.44 (s, 1H), 7.31 (t, J = 7.5 Hz, 2H), 7.21 (t, J = 7.3 Hz, 1H), 7.14 (d, J = 7.2 Hz, 2H), 6.85–6.77 (m, 4H), 5.80 (q, J = 7.0 Hz, 1H), 3.68 (s, 3H), 3.44–3.31 (m, 4H), 2.75–2.71 (m, 4H), 1.85 (d, J = 7.1 Hz, 3H). ^{13}C NMR (100 MHz, DMSO-d_6) δ 159.8, 153.9, 145.3, 142.2, 137.6, 129.2 (2C), 128.4, 128.2, 126.7 (2C), 125.6, 118.7 (2C), 114.7 (2C), 56.1 (2C), 55.6 (2C), 50.1 (2C), 21.6. HRMS calcd for $C_{23}H_{27}N_4O_2$, $[M + H]^+$, 391.2134; found 391.2127.

*4.8.13. (R)-(4-(2-methoxyphenyl)piperazin-1-yl)(1-(1-phenylethyl)-1H-imidazol-5-yl)methanone (**15m**)*

Light white solid; yield: 70.1%; ^{1}H NMR (400 MHz, DMSO-d_6) δ 8.12 (s, 1H), 7.31 (t, J = 7.0 Hz, 2H), 7.22 (t, J = 7.0 Hz, 1H), 7.18 (s, 1H),

7.11 (d, $J = 7.2$ Hz, 2H), 7.01–6.81 (m, 3H), 6.73 (d, $J = 7.5$ Hz, 1H), 5.79 (q, $J = 6.5$ Hz, 1H), 3.75 (s, 3H), 3.45–3.31 (m, 4H), 2.76–2.65 (m, 4H), 1.83 (d, $J = 6.8$ Hz, 3H). ^{13}C NMR (100 MHz, DMSO-d_6) δ 160.8, 152.4, 143.1, 141.0, 138.1, 131.1, 129.1 (2C), 128.1, 126.6 (2C), 125.4, 123.4, 121.2, 118.7, 112.3, 55.8 (2C), 55.6 (2C), 50.4 (2C), 21.7. HRMS calcd for $C_{23}H_{27}N_4O_2$, $[M + H]^+$, 391.2134; found 391.2134.

4.8.14. (R)-(4-cyclopropyl-3,4-dihydroquinoxalin-1(2H)-yl)(1-(1-phenylethyl)-1H-imidazol-5-yl)methanone (**15n**)

Light white solid; yield: 65.2%; ^{1}H NMR (300 MHz, DMSO-d_6) δ 8.11 (s, 1H), 7.38–7.25 (m, 3H), 7.12 (d, $J = 7.0$ Hz, 3H), 6.98 (dd, $J = 12.0$, 4.9 Hz, 1H), 6.90 (s, 1H), 6.59 (d, $J = 7.5$ Hz, 1H), 6.43 (t, $J = 7.6$ Hz, 1H), 5.76 (q, $J = 7.1$ Hz, 1H), 4.06–3.90 (m, 1H), 3.43–3.39 (m, 1H), 3.28–3.23 (m, 1H), 2.93–2.89 (m, 1H), 2.44–2.33 (m, 1H), 1.76 (d, $J = 7.1$ Hz, 3H), 0.84–0.78 (m, 2H), 0.57–0.47 (m, 2H). ^{13}C NMR (100 MHz, DMSO-d_6) δ 159.9, 142.4, 139.6, 137.9, 132.9, 128.7 (2C), 127.8, 126.0 (2C), 125.7, 125.6, 124.9, 123.7, 115.9, 112.9, 54.9, 54.8, 48.1, 31.1, 21.18, 7.9, 7.5. HRMS calcd for $C_{23}H_{25}N_4O$, $[M + H]^+$, 373.2028; found 373.2021.

4.8.15. (R)-(3,4-dihydroquinolin-1(2H)-yl)(1-(1-phenylethyl)-1H-imidazol-5-yl)methanone (**15o**)

Light white solid; yield: 64.8%; ^{1}H NMR (400 MHz, DMSO-d_6) δ 8.11 (s, 1H), 7.40–7.32 (m, 2H), 7.32–7.26 (m, 1H), 7.18 (d, $J = 7.2$ Hz, 2H), 7.14 (d, $J = 7.5$ Hz, 1H), 6.99 (t, $J = 7.1$ Hz, 1H), 6.86 (t, $J = 7.3$ Hz, 1H), 6.79 (s, 1H), 6.47 (d, $J = 8.0$ Hz, 1H), 5.89 (q, $J = 7.1$ Hz, 1H), 3.84 (dt, $J = 12.4$, 6.1 Hz, 1H), 3.41 (ddd, $J = 12.8$, 7.4, 5.5 Hz, 1H), 2.77–2.58 (m, 2H), 1.83 (d, $J = 7.2$ Hz, 3H), 1.77–1.58 (m, 2H). ^{13}C NMR (100 MHz, DMSO-d_6) δ 161.1, 142.4, 138.6, 137.9, 132.9, 131.2, 128.7 (2C), 128.6, 127.8, 126.2, 126.2 (2C), 125.3, 124.5, 124.3, 54.8, 44.7, 25.9, 23.4, 21.2. HRMS calcd for $C_{21}H_{22}N_3O$, $[M + H]^+$, 332.1763; found 332.1760.

4.8.16. (R)-(2,3-dihydro-4H-benzo[b][1,4]oxazin-4-yl)(1-(1-phenylethyl)-1H-imidazol-5-yl)methanone (**15p**)

Light white solid; yield: 69.1%; ^{1}H NMR (400 MHz, DMSO-d_6) δ 8.20 (s, 1H), 7.33 (t, $J = 7.3$ Hz, 2H), 7.28 (d, $J = 7.1$ Hz, 1H), 7.24 (s, 1H), 7.19 (d, $J = 8.0$ Hz, 1H), 7.14 (d, $J = 7.2$ Hz, 2H), 7.02–6.94 (m, 1H), 6.87–6.81 (m, 1H), 6.73 (t, $J = 7.7$ Hz, 1H), 5.86 (q, $J = 7.1$ Hz, 1H), 4.21–4.12 (m, 1H), 3.92–3.83 (m, 1H), 3.68–3.47 (m, 2H), 1.85 (d, $J = 7.1$ Hz, 3H). ^{13}C NMR (100 MHz, DMSO-d_6) δ 160.3, 145.9, 142.6, 138.8, 133.6, 128.7 (2C), 127.8, 126.0 (2C), 125.4, 125.2, 125.1, 123.7, 119.6, 117.0, 65.4, 54.9, 44.1, 21.3. HRMS calcd for $C_{20}H_{19}N_3O_2Na$, $[M + Na]^+$, 356.1375; found 356.1381.

4.9. General procedure for the synthesis of compounds **17a-f**

To a solution of ethyl 1*H*-imidazole-5-carboxylate (1 equiv) **16 and** the substituted benzyl bromide (1 equiv) in Tetrahydrofuran was added 10%NaOH and tetra-*n*-butylammonium bromide (0.2 equiv) at 0 °C. The reaction was stirred for 6–8 h and was then concentrated under reduced pressure. The residue was extracted with EtOAc and then brine. The organic phase was dried over Na_2SO_4 overnight and and the solvent was removed *in vaccuo*. The crude product was purified by silica gel column chromatography to yield the target product **17a-f**.

4.9.1. Ethyl 1-(2,4-dichlorobenzyl)-1H-imidazole-5-carboxylate (**17d**)

^{1}H NMR (400 MHz, DMSO-d_6) δ 8.08 (s, 1H), 7.77 (d, $J = 0.8$ Hz, 1H), 7.70 (d, $J = 2.1$ Hz, 1H), 7.38 (dd, $J = 8.4$, 2.1 Hz, 1H), 6.52 (d, $J = 8.4$ Hz, 1H), 5.59 (s, 2H), 4.15 (q, $J = 7.1$ Hz, 2H), 1.16 (t, $J = 7.1$ Hz, 3H).

4.9.2. Ethyl 1-(2,5-dichlorobenzyl)-1H-imidazole-5-carboxylate (**17e**)

^{1}H NMR (400 MHz, DMSO-d_6) δ 8.09 (s, 1H), 7.78 (d, $J = 0.8$ Hz, 1H), 7.57 (d, $J = 8.5$ Hz, 1H), 7.43 (dd, $J = 8.5$, 2.5 Hz, 1H), 6.49 (d, $J = 2.5$ Hz, 1H), 5.61 (s, 2H), 4.16 (q, $J = 7.1$ Hz, 2H), 1.16 (t, $J = 7.1$ Hz, 3H).

4.10. General procedure for the synthesis of compounds **18 a-f**

Sodium hydroxide (2 N) was added to a solution of intermediate **17a-f** (1 equiv.) in methanol at ambient temperature. The reaction mixture was stirred for 6 h and the methanol was removed by rotary evaporation. The resultant mixture was adjusted to pH = 5–6 with 1 N HCl solution. The precipitated white solid was collected by filtration and dried to give the **18a-f**.

4.11. General procedure for the synthesis of compounds **19a-f**

HATU (1.1 equiv.) and DIEA (2 equiv.) were added to a solution of the intermediate acid compound **18a-f** (1 equiv.) and *1-Cyclopropyl-1,2,3,4-tetrahydro-quinoxaline* **12** (1 equiv.) in anhydrous DMF. The solution was heated to 70 °C for 6 h and then cooled to room temperature. The reaction mixture was poured into ice water, and the resulting solid was filtered. The crude product was purified by silica gel column chromatography to give the target product ***19a-f.***

4.11.1. (1-benzyl-1H-imidazol-5-yl)(4-cyclopropyl-3,4-dihydroquinoxalin-1(2H)-yl)methanone (**19a**)

Light white solid; yield: 73.1%; ^{1}H (400 MHz, DMSO-d_6) δ 7.98 (s, 1H), 7.39–7.24 (m, 3H), 7.13 (d, $J = 7.4$ Hz, 3H), 6.99 (t, $J = 7.7$ Hz, 1H), 6.88 (s, 1H), 6.66 (d, $J = 7.6$ Hz, 1H), 6.45 (t, $J = 7.5$ Hz, 1H), 5.35 (s, 2H), 3.74 (t, $J = 5.2$ Hz, 2H), 3.12 (t, $J = 5.3$ Hz, 2H), 2.40 (ddd, $J = 10.1$, 6.7, 3.7 Hz, 1H), 0.81 (q, $J = 6.5$ Hz, 2H), 0.59–0.46 (m, 2H). ^{13}C NMR (100 MHz, DMSO-d_6) δ 159.8, 140.9, 139.5, 137.5, 133.5, 128.7 (2C), 127.8, 127.3 (2C), 125.6, 125.0, 124.9, 123.7, 115.9, 113.0, 48.6, 48.1, 43.0, 31.2, 7.7 (2C). HRMS calcd for $C_{22}H_{23}N_4O$, $[M + H]^+$, 359.1872; found 359.1872.

4.11.2. (4-cyclopropyl-3,4-dihydroquinoxalin-1(2H)-yl)(1-(4-fluorobenzyl)-1H-imidazol-5-yl)methanone (**19b**)

Light white solid; yield: 71.3%; ^{1}H NMR (400 MHz, DMSO-d_6) δ 7.98 (s, 1H), 7.27–7.10 (m, 5H), 7.00 (t, $J = 7.8$ Hz, 1H), 6.88 (s, 1H), 6.71–6.63 (m, 1H), 6.46 (t, $J = 7.5$ Hz, 1H), 5.34 (s, 2H), 3.75 (t, $J = 5.4$ Hz, 2H), 3.14 (t, $J = 5.3$ Hz, 2H), 2.43–2.36 (m, 1H), 0.82 (q, $J = 6.4$ Hz, 2H), 0.60–0.49 (m, 2H). ^{13}C NMR (100 MHz, DMSO-d_6) δ 159.8, 140.9, 139.6, 133.8, 133.7, 133.6, 129.7, 129.6, 125.7, 124.9, 124.9, 123.8, 115.9, 115.6, 115.4, 113.0, 48.1, 47.9, 43.0, 31.2, 7.7 (2C). HRMS calcd for $C_{22}H_{22}FN_4O$, $[M + H]^+$, 377.1778; found 377.1792.

4.11.3. (1-(2-chlorobenzyl)-1H-imidazol-5-yl)(4-cyclopropyl-3,4-dihydroquinoxalin-1(2H)-yl)methanone (**19c**)

Light white solid; yield: 66.7%; ^{1}H NMR (400 MHz, DMSO-d_6) δ 7.98 (s, 1H), 7.25–7.10 (m, 5H), 7.04–6.96 (m, 1H), 6.88 (s, 1H), 6.67 (d, $J = 7.3$ Hz, 1H), 6.46 (t, $J = 7.3$ Hz, 1H), 5.34 (s, 2H), 3.75 (t, $J = 5.4$ Hz, 2H), 3.14 (t, $J = 5.4$ Hz, 2H), 2.44–2.36 (m, 1H), 0.85–0.78 (m, 2H), 0.58–0.52 (m, 2H). ^{13}C NMR (100 MHz, DMSO-d_6) δ 159.5, 141.6, 139.6, 135.1, 133.6, 131.7, 129.5, 128.4, 127.6, 125.9, 125.7, 125.1, 124.8, 123.8, 116.0, 113.0, 48.1, 46. 7, 43.2, 31.2, 7.8 (2C). HRMS calcd for $C_{22}H_{22}ClN_4O$, $[M + H]^+$, 393.1482; found 393.1476.

4.11.4. (4-cyclopropyl-3,4-dihydroquinoxalin-1(2H)-yl)(1-(2,4-dichlorobenzyl)-1H-imidazol-5-yl)methanone (**19d**)

Light white solid; yield: 69.4%; ^{1}H NMR (400 MHz, DMSO-d_6) δ 7.93 (s, 1H), 7.67 (d, $J = 2.1$ Hz, 1H), 7.42 (dd, $J = 8.4$, 2.1 Hz, 1H), 7.16 (d, $J = 8.2$ Hz, 1H), 7.01 (dd, $J = 11.3$, 4.2 Hz, 1H), 6.96 (s, 1H), 6.88 (d, $J = 7.9$ Hz, 1H), 6.82 (d, $J = 8.4$ Hz, 1H), 6.52 (t, $J = 7.6$ Hz, 1H), 5.47 (s, 2H), 3.81 (t, $J = 5.3$ Hz, 2H), 3.20 (t, $J = 5.3$ Hz, 2H), 2.46–2.36 (m, 1H), 0.88–0.78 (m, 2H), 0.61–0.50 (m, 2H). ^{13}C NMR (100 MHz, DMSO-d_6) δ 159.4, 141.6, 139.6, 134.3, 133.7, 133.1, 132.7, 129.8, 128.9, 127.7, 125.8, 125.0, 124.8, 123.8, 116.0, 113.0, 48.1, 46.3, 43.1, 31.2, 7.7 (2C).HRMS calcd for $C_{22}H_{21}Cl_2N_4O$, $[M + H]^+$, 427.1092; found

427.1075.

4.11.5. (4-cyclopropyl-3,4-dihydroquinoxalin-1(2H)-yl)(1-(2,5-dichlorobenzyl)-1H-imidazol-5-yl)methanone (19e)

Light white solid; yield: 72.1%; ^{1}H NMR (400 MHz, DMSO-d_6) δ 7.95 (s, 1H), 7.55 (d, J = 8.5 Hz, 1H), 7.44 (dd, J = 8.5, 2.5 Hz, 1H), 7.16 (d, J = 7.9 Hz, 1H), 7.03 (t, J = 7.7 Hz, 1H), 6.95 (s, 1H), 6.87 (d, J = 7.8 Hz, 1H), 6.76 (d, J = 2.4 Hz, 1H), 6.52 (t, J = 7.4 Hz, 1H), 5.49 (s, 2H), 3.82 (t, J = 5.4 Hz, 2H), 3.25 (t, J = 5.4 Hz, 2H), 2.46–2.36 (m, 1H), 0.83 (q, J = 6.5 Hz, 2H), 0.62–0.51 (m, 2H). ^{13}C NMR (100 MHz, DMSO-d_6) δ 159.4, 141.7, 139.7, 137.4, 133.7, 132.1, 131.2, 130.4, 129.3, 127.9, 125.9, 124.9, 124.8, 123.8, 115.9, 113.1, 48.2, 46.5, 43.0, 31.2, 7.7 (2C).HRMS calcd for $C_{22}H_{21}Cl_2N_4O$, $[M + H]^+$, 427.1092; found 427.1082.

4.11.6. (4-cyclopropyl-3,4-dihydroquinoxalin-1(2H)-yl)(1-(2,4-difluorobenzyl)-1H-imidazol-5-yl)methanone (19f)

Light white solid; yield: 61.6%; ^{1}H NMR (400 MHz, DMSO-d_6) δ 7.92 (s, 1H), 7.33–7.24 (m, 1H), 7.19–6.98 (m, 4H), 6.89 (s, 1H), 6.76 (d, J = 7.3 Hz, 1H), 6.49 (t, J = 7.6 Hz, 1H), 5.41 (s, 2H), 3.78 (t, J = 5.4 Hz, 2H), 3.19 (t, J = 5.3 Hz, 2H), 2.45–2.36 (m, 1H), 0.82 (q, J = 6.5 Hz, 2H), 0.56 (dd, J = 6.4, 3.6 Hz, 2H). ^{13}C NMR (100 MHz, DMSO-d_6) δ 159.5, 141.2, 139.6, 133.3, 131.1, 131.0, 125.7, 125.0, 124.8, 123.7, 120.9, 120.8, 115.9, 113.0, 111.8, 104.2, 56.0, 48.1, 42.5, 31.18, 7.7 (2C). HRMS calcd for $C_{22}H_{21}F_2N_4O$, $[M + H]^+$, 395.1683; found 395.1672.

4.12. Cell-Based TGR5 agonism assay

A lentivirus expressing human TGR5 (NM_001077191.1) and mouse (NM_174985) were obtained from Hanbio Biotechnology Co. Ltd. HEK293T cells were transfected with lentivirus and a stable cell line was isolated using drug selection following standard techniques. LCA and INT-777 was used as reference compounds. The test compounds and reference compounds were prepared in DMSO at stock solutions of 10 mM. TGR5-mediated cAMP generation was assayed using a HTRF (Homogeneous Time-Resolved Fluorescence) detection method (HTRF cAMP dynamic 2 Assay Kit; Cisbio cat # 62AM4PEB) according to the manufacturer's protocol.

4.13. FXR activity assay

Biotinylated SRC1 peptide (5′-biotin-CPSSHSSLTERHKILHRLL-QEGSPS-CONH$_2$) was synthesized by GL Biochem (Shanghai) Ltd. (China). Human FXR ligand binding domain (GST-FXRαLBD) was expressed and purified by Shanghai Shengong Biotechonology (Shanghai, China). The assay mixture contained 10 nM GST- FXRαLBD, 100 nM biotin-SRC1, 0.83 nM Eu-labeled anti-GST, and 41.75 nM Streptavidin-XL665 (Cisbio, USA) in HTRF buffer. The HTRF buffer was composed of 50 mM Hepes pH 7.0, 125 mM KF, 0.125% CHAPS, and 0.05% dry milk. The white 384-well microplates were incubated at room temperature and then read with a CLARIOstar Microplate Reader (BMG LABTECH) and calculated using the equation (665 nm/620 nm) * 10,000.

4.14. Oral Glucose Tolerance Test (OGTT)

Male C57L/6J mice (6–8 weeks old) were obtained from Beijing Vital River Laboratory Animal Technologies Co. Ltd and randomly assigned to 3 groups (n = 8 in each group). Overnight-fasted C57L/6J mice were orally administered the vehicle (0.25% CMC) or test compounds **19d** and **19e** at 30 mg/kg, followed by an oral glucose load (4 g/kg) at 60 min post compound dose. Blood glucose levels were measured via blood drops obtained by clipping the tail of the mice before compound dosing and 0, 15, 30, 60, and 120 min post glucose loading. Blood glucose levels and Glucose AUC were carried out in GraphPad Prism.

4.15. GLP-1 secretion

To examine the in vivo effect of compound **19d** on GLP-1 secretion, vehicle (0.25% CMC) or test compound **19d** at 30 mg/kg was administered orally to overnight-fasted eight-week-old wild-typ (WT) (C57BL/6J) or TGR5$^{-/-}$ mice (TGR5 KO). 1 h later, all of the mice were received an oral glucose (2.0 g/kg) challenge. Blood samples were collected at 5 min after the glucose challenge and placed into eppendorf tubes containing the dipeptidyl peptidase IV (DPP IV) inhibitor with a final concentration of 1% blood samples and 25 mg/mL EDTA to measure serum active GLP-1[7–36 amide] levels.

Declaration of Competing Interest

The authors declare that they have no known competing financial interests or personal relationships that could have appeared to influence the work reported in this paper.

Acknowledgements

This research was supported by the National Natural Science Foundation of China (Grant No. 81970726 and No. 81472232), Henan Provincial Natural Science Foundation (Grant No.182300410323), First Class Discipline Cultivation Project of Henan University (Grant No. 2019YLZDYJ19) and Plan for Scientific Innovation Talent of Henan Province (Grant No. 154100510004), Key Program for Science & Technology from Henan Education Department (Grant No. 21A310001) to W.-D.C., the National Natural Science Foundation of China (Grant No.81903444), China Postdoctoral Science Foundation (Grant No. 2018M640674), Key Science and Technology Program of Henan Province (Grant No. 192102310145) and Henan Postdoctoral Foundation (Grant No. 201902027) to S.Z., Major Scientific and Technological Innovation Project of Hebi to W.L., the National Natural Science Foundation of China (Grant No. 81970551 and No. 81672433) and the Fundamental Research Funds for the Central Universities and Research projects on biomedical transformation of China-Japan Friendship Hospital (Grant No. PYBZ1803) to Y.-D.W.

Appendix A. Supplementary material

Supplementary data to this article can be found online at https://doi.org/10.1016/j.bmc.2020.115972.

References

1 Tiwari A, Maiti P. TGR5: an emerging bile acid G-protein-coupled receptor target for the potential treatment of metabolic disorders. *Drug Discovery Today*. 2009;14:523–530.
2 Zhong Min. TGR5 as a therapeutic target for treating obesity. *Current Top Med Chem*. 2010;10:386–396.
3 Pols TWH, Noriega LG, Nomura M, et al. The bile acid membrane receptor TGR5 as an emerging target in metabolism and inflammation. *J Hepatol*. 2011;54:1263–1272.
4 Guo C, Qi H, Yu YJ, et al. The G-protein-coupled bile acid receptor Gpbar1 (TGR5) inhibits gastric inflammation through antagonizing NF-kappa B signaling pathway. *Front Pharmacol*. 2015;6:287.
5 Fryer RM, Ng KJ, Mazurek SGN, et al. G protein-coupled bile acid receptor 1 stimulation mediates arterial vasodilation through a KCa1.1 (BKCa)-dependent mechanism (vol 348, pg 421, 2014). *J Pharmacol Exp Therapeut*. 2014;349, 174–174.
6 Klindt C, Reich M, Hellwig B, et al. The G protein-coupled bile acid receptor TGR5 (Gpbar1) modulates endothelin-1 signaling in liver. *Cells*. 2019;8:21.
7 Keitel V, Stindt J, Haussinger D. Bile acid-activated receptors: GPBAR1 (TGR5) and other G protein-coupled receptors. *Handb Exp Pharmacol*. 2019;256:19–49.
8 Katsuma S, Hirasawa A, Tsujimoto G. Bile acids promote glucagon-like peptide-1 secretion through TGR5 in a murine enteroendocrine cell line STC-1. *Biochem Biophys Res Commun*. 2005;329:386–390.
9 Ullmer C, Sanchez RA, Sprecher U, et al. Systemic bile acid sensing by G protein-coupled bile acid receptor 1 (GPBAR1) promotes PYY and GLP-1 release. *Br J Pharmacol*. 2013;169:671–684.
10 Watanabe M, Houten SM, Mataki C, et al. Bile acids induce energy expenditure by promoting intracellular thyroid hormone activation. *Nature*. 2006;439:484–489.

11 Zhang XQ, Wall M, Sui ZH, et al. Discovery of orally efficacious tetrahydrobenzimidazoles as TGR5 agonists for type 2 diabetes. *ACS Med Chem Lett*. 2017;8:560–565.
12 Duboc H, Tache Y, Hofmann AF. The bile acid TGR5 membrane receptor: From basic research to clinical application. *Dig Liver Dis*. 2014;46:302–312.
13 Hodge RJ, Nunez DJ. Therapeutic potential of Takeda-G-protein-receptor-5 (TGR5) agonists. Hope or hype? *Diabetes Obes Metab*. 2016;18:439–443.
14 Pellicciari R, Gioiello A, Macchiarulo A, et al. Discovery of 6 alpha-Ethyl-23(S)-methylcholic Acid (S-EMCA, INT-777) as a potent and selective agonist for the TGR5 receptor, a novel target for diabesity. *J Med Chem*. 2009;52:7958–7961.
15 Thomas C, Gioiello A, Noriega L, et al. TGR5-mediated bile acid sensing controls glucose homeostasis. *Cell Metab*. 2009;10:167–177.
16 Evans KA, Budzik BW, Ross SA, et al. Discovery of 3-aryl-4-isoxazolecarboxamides as TGR5 receptor agonists. *J Med Chem*. 2009;52:7962–7965.
17 Herbert MR, Siegel DL, Staszewski L, et al. Synthesis and SAR of 2-aryl-3-amino-methylquinolines as agonists of the bile acid receptor TGR5. *Bioorg Med Chem Lett*. 2010;20:5718–5721.
18 Budzik BW, Evans KA, Wisnoski DD, et al. Synthesis and structure-activity relationships of a series of 3-aryl-4-isoxazolecarboxamides as a new class of TGR5 agonists. *Bioorg Med Chem Lett*. 2010;20:1363–1367.
19 Zou QA, Duan HL, Ning MM, et al. 4-Benzofuranyloxynicotinamide derivatives are novel potent and orally available TGR5 agonists. *Eur J Med Chem*. 2014;82:1–15.
20 Agarwal S, Patil A, Aware U, et al. Discovery of a potent and orally efficacious TGR5 receptor agonist. *ACS Med Chem Lett*. 2016;7:51–55.
21 Agarwal S, Sasane S, Kumar J, et al. Evaluation of novel TGR5 agonist in combination with Sitagliptin for possible treatment of type 2 diabetes. *Bioorg Med Chem Lett*. 2018;28:1849–1852.
22 Duan HL, Ning MM, Chen XY, et al. Design, synthesis, and antidiabetic activity of 4-phenoxynicotinamide and 4-phenoxypyrimidine-5-carboxamide derivatives as potent and orally efficacious TGR5 agonists. *J Med Chem*. 2012;55:10475–10489.
23 Martin RE, Bissantz C, Gavelle O, et al. 2-Phenoxy-nicotinamides are potent agonists at the bile acid receptor GPBAR1 (TGR5). *ChemMedChem*. 2013;8:569–576.
24 Chen T, Reich NW, Bell N, et al. Design of gut-restricted thiazolidine agonists of G protein-coupled bile acid receptor 1 (GPBAR1, TGR5). *J Med Chem*. 2018;61:7589–7613.
25 Nakhi A, McDermott CM, Stoltz KL, et al. 7-Methylation of chenodeoxycholic acid derivatives yields a substantial increase in TGR5 receptor potency. *J Med Chem*. 2019;62:6824–6830.
26 Sepe V, Renga B, Festa C, et al. Modification on ursodeoxycholic acid (UDCA) scaffold. Discovery of bile acid derivatives as selective agonists of cell-surface G-protein coupled bile acid receptor 1 (GP-BAR1). *J Med Chem*. 2014;57:7687–7701.
27 Piotrowski DW, Futatsugi K, Warmus JS, et al. Identification of tetrahydropyrido 4,3-d pyrimidine amides as a new class of orally bioavailable TGR5 agonists. *ACS Med Chem Lett*. 2013;4:63–68.